ELSEVIER

International Journal of Mass Spectrometry 216 (2002) 249–255

International Journal of Mass Spectrometry

www.elsevier.com/locate/ijms

# Mass and photoelectron spectrometer for studying field-induced ionization of molecules

Chengyin Wu, Haizhen Ren, Tingting Liu, Ri Ma, Hong Yang, Hongbing Jiang, Qihuang Gong*

*Department of Physics, State Key Laboratory for Mesoscopic Physics, Peking University, Beijing 100871, PR China*

Received 25 January 2002; accepted 5 March 2002

**Abstract**

We present a simple experimental apparatus, a time-of-flight mass spectrometer (TOFMS) and a photoelectron spectrometer (PES), for studying the ionization of molecules induced by intense femtosecond laser fields. Both the angular and the kinetic energy distributions of the ions and the photoelectrons can be precisely measured. As an example, the dynamics data for $CS_2$ were measured using the spectrometer, and the results revealed that field-induced ionization played the main contribution for $CS_2$ in an intense femtosecond laser field. (Int J Mass Spectrom 216 (2002) 249–255) © 2002 Published by Elsevier Science B.V.

*Keywords:* Ion spectroscopy; Photoelectron spectroscopy; Intense femtosecond laser; Field ionization; Angular distribution

## 1. Introduction

Femtosecond laser mass spectra (FLMS) can lead to enhanced parent molecular signals in comparison to nanosecond laser excitation which indicates that FLMS has considerable potential applications in chemical analysis [1]. Therefore, the ionization of molecules in an intense femtosecond laser field has attracted particular attention in recent years [1–12]. Most of the reports describe a time-of-flight mass spectrometer (TOFMS) coupled with a femtosecond laser amplifier for recording of the mass spectra of the ions produced by the intense femtosecond laser pulses at different intensities. They also present the dependence of the ion intensity on the laser pulse intensity. However, the relationship between the ion and the laser intensity cannot provide enough dynamical information for determining of the precise ionization mechanism of the molecules in an intense laser field, especially when the laser intensity is $10^{13}$–$10^{15}$ W/cm$^2$. For example, Ledingham and coworkers [6,7] found that the dependence of the ion intensity on the laser intensity could be described by multiphoton ionization equations when they studied the ionization of $NO_2$ interacting with intense femtosecond laser pulses. Talebpour et al. [11] reported that multiphoton ionization of inner-valence electrons was able to satisfactorily predict the laser intensity dependence of the ion intensity when they studied the interaction mechanism of intense femtosecond laser pulses with ethylene. Wu et al. [12] reported that field ionization mechanism could also predict

* Corresponding author. E-mail: qhgong@pku.edu.cn

1387-3806/02/$ – see front matter 
*PII* S1387-3806(02)00639-5

the laser dependence of the ion intensity well when they studied the ionization of aliphatic ketones in intense laser field. From the above discussions, we know that more data are needed to determine the ionization mechanism of molecules in an intense laser field.

In addition to the TOFMS, the PES is another useful tool to elucidate the ionization process of molecules in an intense laser field because the photoelectron spectra contain much dynamical information about the ionization processes [3,13,14]. For example, a broad distribution extending above the laser's ponderomotive potential was observed in the field ionization regime [13]. While in the multiphoton ionization regime, a series of discrete peaks originated from above threshold ionization was observed [14]. However, the study of the photoelectron produced by the interaction of molecules with intense laser field is scarce. The study of both the ions and the photoelectrons under the similar laser condition is even scarce.

In this article, we present simple TOFMS and PES to study the ionization of molecules in an intense laser field. The simultaneously obtained dynamics data for both the ions and the photoelectrons are proven to be helpful for investigating the ionization mechanism of molecules in intense laser field.

## 2. Experimental apparatus

### *2.1. Time-of-flight mass spectrometer and photoelectron spectrometer (TOFMS–PES)*

The schematic diagram of the TOFMS and PES is shown in Fig. 1. The field-free drift region has a length of 35 cm and the inner wall of the entire vacuum chamber is wrapped up with μ-metal to shield the external magnetic fields. The spectrometer is designed to measure the laser induced photoelectron and mass spectra of molecules in the field ionization regime.

The photoelectron spectra in the field ionization regime have been well described by a two-step model [15–18]. Firstly, the electrons are ejected through tunneling to near-zero kinetic energy states. Secondly, the still-present strong electric field forces the photoelectron to oscillate along the laser polarization vector. Thus, the momentums of the photoelectrons mainly distribute along the laser polarization vector. Therefore, when the laser polarization vector is parallel to the direction of the detector, using the above stated conventional linear mass spectrometer based on the Wiely–McLaren configuration, we can collect the photoelectron with high efficiency without applying any magnetic or electric field to guide the photoelectrons

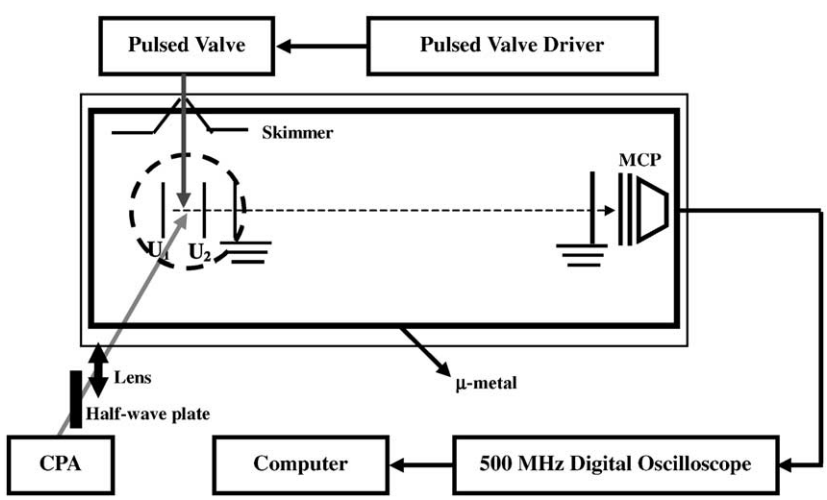


Fig. 1. Schematic diagram of the experimental apparatus. It mainly contains a CPA laser, a home-built TOFMS, and a PES.

to the detector. While in the multiphoton ionization regime, the photoelectron is emitted from all directions. In order to increase the electron collection efficiency, an inhomogeneous magnetic field parallel to the flight axis is required to guide mostly all photoelectrons to the detector [19–22].

When the mass spectra are measured, proper positive voltages $U_1$ and $U_2$ are chosen to meet the requirement of the first spatial focus to pursue the high mass resolution. The optimum mass resolution can reach 116 at $m/z = 58$. When the photoelectrons are collected, both $U_1$ and $U_2$ are set to 0. Thus, the photoelectron could fly free to the field-free drift tube. The kinetic energy distribution of the photoelectrons can be calculated through the time that is necessary for the electron to reach the detector. Rotating the laser polarization vector and detecting the ion and the photoelectron intensity at different laser polarization angle, we can measure the angular distribution of the ions and the photoelectrons.

A dual MCP is used to detect these charged particles. The voltage between the first MCP surface and the ground is set to 300 V to decelerate the ions and accelerate the photoelectrons. Thus, the kinetic energy of the charged particles is near 400 eV before striking the MCP surface. At this kinetic energy range, MCP has the maximum amplified efficiency for these charged particles.

Gaseous samples are introduced into the chamber via a pulsed valve (Parker Inc., USA). The base pressure is about $2 \times 10^{-5}$ Pa that is pumped by a turbo molecular pump (600 L/s). The chamber pressure is maintained between $2 \times 10^{-4}$ and $8 \times 10^{-4}$ Pa when gaseous molecules are introduced. The signal is recorded using a 500 MHz digital oscilloscope (H.P. Inc., USA) and then transferred to a PC for storage and analysis.

In general, we can obtain the angular and the kinetic energy distributions for both ions and photoelectrons with this simple experimental apparatus. The apparatus is characterized by at least two advantageous features. The first one is that the operation is very simple. We only change the voltages of $U_1$ and $U_2$ when we measure the mass and the photoelectron spectra. The second one is that the angular distributions of the ions and photoelectrons are not distorted. There are no electrostatic and magnetic fields in the ionization zone when we measure the angular distribution of these charged particles.

### 2.2. Femtosecond laser system

A Ti:Sapphire chirped pulse amplifier (CPA) system (TSA-10, Spectra-Physics Inc., USA) delivers laser pulses with wavelength of 810 nm, pulse duration of 110 fs at a repetition rate of 10 Hz. The maximum pulse energy is 10 mJ. The amplified laser beam is focused into the chamber of a TOF spectrometer by a lens with focus-length of 150 mm. A half-wave plate is used to rotate the laser linear polarization vector and a quarter-wave plate to produce circular polarized laser.

## 3. Applications

The validity of the above TOFMS–PES apparatus was tested by the study of the ionization of $CS_2$ in an intense femtosecond laser field.

### 3.1. Ion spectroscopy

Fig. 2 shows the TOF mass spectra of $CS_2$ produced by 810 nm, 110 fs laser pulse at intensity of $2 \times 10^{15}$ W/cm$^2$. The laser polarization is horizontal in the upper trace and vertical in the middle trace and circular in the lower trace. It was noted that the intact molecular ions $CS_2^+$ and $CS_2^{2+}$ had similar intensity and shape in the mass spectra for both vertical and horizontal polarized laser pulses. In addition to the above intact molecular ions, some singly and highly charged atomic ions $S^{m+}$ ($m = 1$–5) and $C^{n+}$ ($n = 1$–3) were also generated and split into double peaks, which manifested that these atomic ions were produced through Coulomb explosion of the highly charged molecular ions [23,24]. Moreover, only $S^{m+}$ ($m = 1$–5) and weak $C^+$ were present and $C^{2+}$ and $C^{3+}$ were almost entirely missing in the horizontal polarization mass spectra. While in the vertical

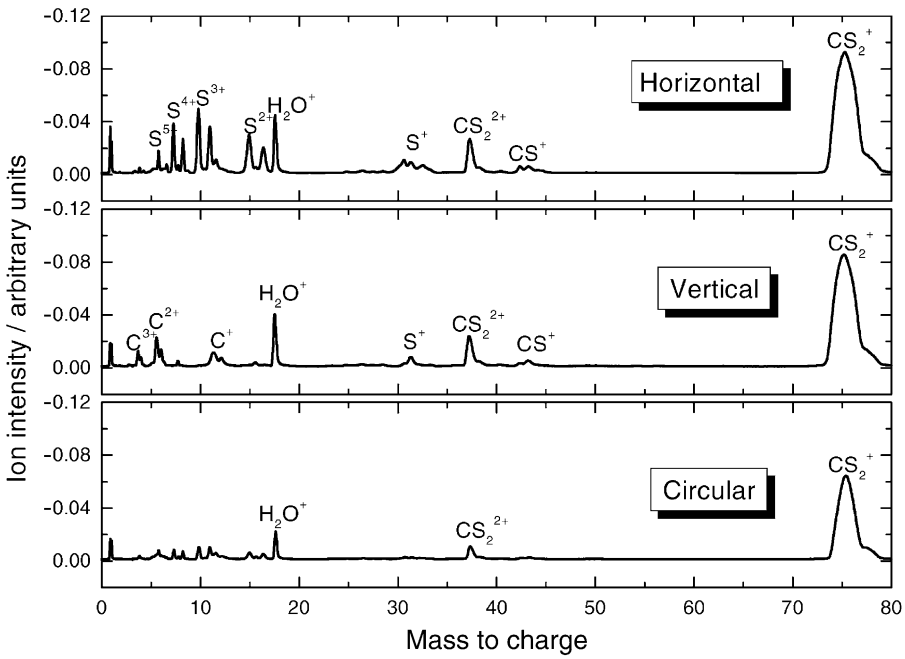


Fig. 2. TOF mass spectra of $CS_2$ induced by 810 nm, 110 fs laser pulses at intensity of $2 \times 10^{15}$ W/cm$^2$. The laser polarization is horizontal in the upper trace, vertical in the middle trace, and circular in the lower trace.

polarization mass spectra, only $C^{n+}$ ($n = 1$–3) and $S^+$ were present and $S^{m+}$ ($m = 2$–5) were almost entirely missing. The facts indicated that the highly charged molecular ions are aligned by the intense laser field prior to explosions. Moreover, the momentums are distributed mainly along the laser polarization vector for $S^{m+}$ and vertical to the laser polarization vector for $C^{n+}$.

It was also obvious from Fig. 2 that the suppression of ionization occurred for circular polarized laser. This fact agreed with the result predicted by field ionization models [3,12,25]. According to these field ionization models of molecules, the field ionization probability is the tunneling efficiency of the electron through the barrier formed by the molecular potential and the instantaneous electric field of the laser. The key factor of field ionization is that the barrier must remain static for long enough to allow the electron to penetrate the barrier. For circular polarized laser, the laser electric field vector is circumrotating. Thus, the electrons do not have enough time to penetrate the barrier before the laser electric vector changes. Therefore, the ionization probability is smaller for the circular polarized laser compared with the linear polarized laser at the same laser intensity.

By measuring the differences in the TOF of the split peaks in the mass spectra, we can obtain the kinetic energy of these ions. The following equation determines the kinetic energy of the ions with splitting peaks [26]:

$$E_{\text{Kinetic energy}} = \frac{(U_1 - U_2)^2}{8md^2} q^2 \Delta t^2 \quad (1)$$

where $m$ is the mass of the ion, $U_1$ is the potential of the repeller plate, $U_2$ is that for the first acceleration plate, $d$ is the distance between these plates, $q$ is the charge of the ion, and $\Delta t$ is the difference in the arrival times between the forward and backward ejected ions. The experimental measured kinetic energies for $S^{m+}$ ($m = 1$–5) and $C^{n+}$ ($n = 1$–3) at laser intensity of $2 \times 10^{15}$ W/cm$^2$ were listed in Table 1. It can be seen that the kinetic energies for the ions are very large, which reaches several tens electron volts.

Table 1
Measured kinetic energies and FWHMs of the angular distributions for $S^{m+}$ ($m$ = 1–5) and $C^{n+}$ ($n$ = 1–3) at intensity of $2 \times 10^{15}$ W/cm$^2$

| Atomic ions | Kinetic energy (eV) | FWHM (°) |
|---|---|---|
| $C^+$ | 4.3 | 64.8 |
| $C^{2+}$ | 11.6 | 51.7 |
| $C^{3+}$ | 15.1 | 43.1 |
| $S^+$ | 4.0 | 56.1 |
| $S^{2+}$ | 18.2 | 52.2 |
| $S^{3+}$ | 39.6 | 43.7 |
| $S^{4+}$ | 65.6 | 39.7 |
| $S^{5+}$ | 91.3 | 32.4 |

By rotating the half-wave plate, we can change the linear polarization vector of the laser beam, which corresponds to detecting the charged particles from different directions relative to the laser polarization vector because the detector is fixed. Thus, we obtained the angular distribution of the ions through measuring the ions' intensities at different laser polarization angles. In order to avoid the distortion by the extracting electric field in the ionization zone, we applied no electric field in the ionization zone when we measured the angular distribution of the ions. It would be interesting to know the angular distribution of the ions with no electric field applied to the ionization zone. The molecular ions $CS_2^+$ and $CS_2^{2+}$ exhibited strong isotropic angular distributions. While the atomic ions $S^{m+}$ ($m$ = 1–5) and $C^{n+}$ ($n$ = 1–3) show highly anisotropic angular distributions. $S^{m+}$ has the maximum intensities along the laser polarization and $C^{n+}$ has the maximum intensities vertical to the laser polarization. The angular distribution for both the molecular and the atomic ions were consistent with that reported by other groups [23,27,28]. We also measured the full width at half maximum (FWHM) for $S^{m+}$ ($m$ = 1–5) and $C^{n+}$ ($n$ = 1–3), which were listed in Table 1. It is obvious that the FWHM of the angular distribution for $S^{m+}$ and $C^{n+}$ become narrower as a function of charge state. The result agreed with that reported by Couris who measured the angular distribution of $CS_2$ under the condition of zero-field in the ionization zone [27]. However, Glasgow group [23] reported that the measured FWHM values were equal for all sulfur ions. The conflict between the results of Glasgow group and our group and Couris' group may be due to the extracted field in the ionization zone that distorted the angular distributions of the ions.

### 3.2. Photoelectron spectroscopy

The photoelectron spectrum for $CS_2$ is shown in Fig. 3 after excitation by 810 nm, 110 fs laser pulse at a laser intensity of $2 \times 10^{15}$ W/cm$^2$. It is obvious that there are no discernible features other than a broad distribution. The photoelectron kinetic energy distribution extends to several tens of eV. From the above discussion in Section 2, we know that the photoelectrons were produced through two steps according to the two-step model [15–18]. Firstly, the electrons were ionized through tunneling to near-zero kinetic energy states. Secondly, the still-present strong electric field forces the photoelectron to oscillate along the laser polarization vector and the photoelectron obtains a certain kinetic energy. Because the tunneling time of electron through the barrier formed by the molecular potential and the instantaneous electric field of the laser can not be precisely determined, the kinetic energy of the photoelectron in the laser electric field is indeterminate, which agreed with our measured photoelectron spectrum that exhibited a featureless broad distribution. The average kinetic energy of an electron in the laser field is determined by the ponderomotive potential $U_P$ [26], which is given by:

$$U_P = \frac{e^2\varepsilon^2}{4m\omega^2} = 9.33 \times 10^{-14} I\lambda^2 \quad (2)$$

where $\varepsilon$ is the electric field strength, $I$ (W/cm$^2$) is the laser intensity, and $\lambda$ (μm) is the wavelength. The ponderomotive potential can reach tens of eV at $2 \times 10^{15}$ W/cm$^2$, which qualitatively agreed with our experimental measured result.

Fig. 4 shows the angular distribution of the photoelectron at a laser intensity of $2 \times 10^{15}$ W/cm$^2$. It is markedly anisotropic, peaking along the laser polarization. This fact is also consistent with predictions of the field ionization mechanism. According to two-step field ionization model [15–18], the photoelectron

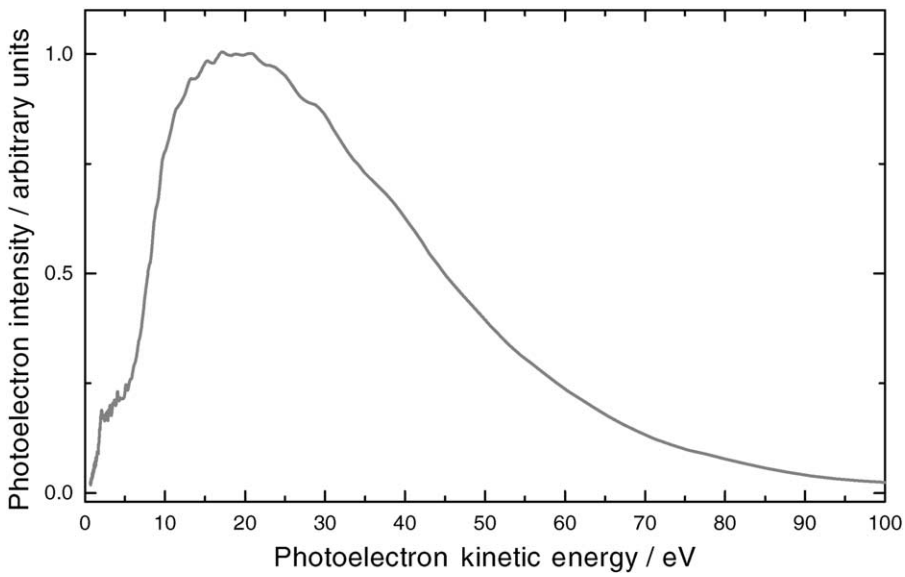


Fig. 3. The photoelectron kinetic energy spectrum of $CS_2$ induced by 810 nm, 110 fs laser pulses at laser intensity of $2 \times 10^{15}$ W/cm$^2$. The kinetic energy of the photoelectron exhibits a featureless broad distribution extending above the laser's ponderomotive potential.

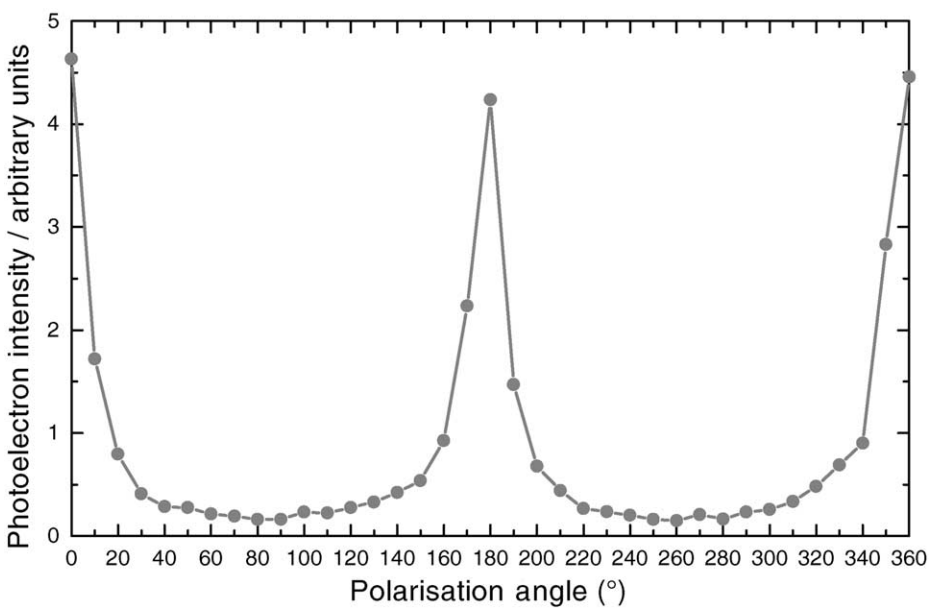


Fig. 4. Angular distributions for the photoelectrons at laser intensity of $2 \times 10^{15}$ W/cm$^2$. It is obvious that the angular distribution of the photoelectron is markedly anisotropic and mainly distributed along the laser polarization vector.

obtained the momentum during the vibration processes forced by the laser electric field. Therefore, the photoelectron momentum is distributed mainly along the laser polarization vector.

## 4. Conclusion

Using a home-made TOFMS and PES, we obtained both the mass and the photoelectron spectra of molecules in field ionization regime. The kinetic energy distributions for both the ions and the photoelectrons were determined from the mass and the photoelectron spectra, respectively. Combined with the rotation of the polarization of a linear polarized laser, we determined precisely the angular distribution of the ions and the photoelectrons. These dynamics data agreed excellently with the predictions of the field ionization mechanism. This fact indicates that our home-designed simple TOF spectrometer is a powerful tool for investigation of the laser–molecule interaction in field ionization regime.

## Acknowledgements

The work was supported by the National Key Basic Research Special Foundation (NKBRSF) under Grant No. G1999075207 and National Natural Science Foundation of China under Grant No. 90101027, 19884001 and 19525412 and China Postdoctoral Science Foundation.

## References

[1] K.W.D. Ledingham, C. Kosmidis, S. Georgiou, S. Couris, R.P. Singhal, Chem. Phys. Lett. 247 (1995) 555.
[2] K.F. Willey, C.L. Brummel, N. Winograd, Chem. Phys. Lett. 267 (1997) 359.
[3] M.J. Dewitt, R.J. Levis, Phys. Rev. Lett. 81 (1998) 5101.
[4] M.J. Dewitt, R.J. Levis, J. Chem. Phys. 110 (1999) 11368.
[5] R.J. Levis, M.J. Dewitt, J. Phys. Chem. A 103 (1999) 6493.
[6] R.P. Singhal, H.S. Kilic, K.W.D. Ledingham, C. Kosdimis, T. McCanny, A.J. Langley, W. Shaikh, Chem. Phys. Lett. 253 (1996) 81.
[7] R.P. Singhal, H.S. Kilic, K.W.D. Ledingham, T. McCanny, W.X. Peng, D.J. Smith, C. Kosmidis, A.J. Langley, P.F. Taday, Chem. Phys. Lett. 292 (1998) 643.
[8] K.W.D. Ledingham, R.P. Singhal, Int. J. Mass Spectrom. Ion Process 163 (1997) 149.
[9] M. Castillejo, S. Couris, E. Koudoumas, M. Martin M, Chem. Phys. Lett. 289 (1998) 303.
[10] M. Castillejo, S. Couris, E. Koudoumas, M. Martin M, Chem. Phys. Lett. 308 (1999) 373.
[11] A. Talebpour, A.D. Bondrauk, J. Yang, S.L. Chin, Chem. Phys. Lett. 313 (1999) 789.
[12] C.Y. Wu, Y.J. Xiong, N. Ji, Y. He, Z. Gao, F.A. Kong, J. Phys. Chem. A 105 (2001) 374.
[13] E. Mevel, P. Breger, R. Trainham, G. Petite, P. Agostini, A. Migus, J.P. Chambaret, A. Antonetti, Phys. Rev. Lett. 70 (1993) 406.
[14] P. Agostini, F. Fabre, G. Mainfray, G. Petite, N.K. Rahman, Phys. Rev. Lett. 42 (1979) 1127.
[15] P.B. Corkum, Phys. Rev. Lett. 71 (1993) 1994.
[16] G.G. Paulus, W. Becker, W. Nicklich, H. Walther, J. Phys. B: At. Mol. Opt. Phys. 27 (1994) L703.
[17] G.G. Paulus, W. Nicklich, H.L. Xu, P. Lambropoulos, H. Walther, Phys. Rev. Lett. 72 (1994) 2851.
[18] M.J. Nandor, M.A. Walker, L.D. Van Woerkom, J. Phys. B: At. Mol. Opt. Phys. 31 (1998) 4617.
[19] P. Kruit, F.H. Read, J. Phys. E 16 (1983) 313.
[20] O. Cheshnovsky, S.H. Yang, C.L. Pettiette, M.J. Craycraft, R.E. Smalley, Rev. Sci. Instrum. 58 (1987) 2131.
[21] H. Handschuh, G. Gantefor, W. Eberhardt, Rev. Sci. Instrum. 66 (1995) 3838.
[22] L. Lehr, R. Weinkauf, E.W. Schlag, Int. J. Mass Spectrom. 206 (2001) 191.
[23] P. Graham, K.W.D. Ledingham, R.P. Singhal, T. McCanny, S.M. Hankin, X. Fang, D.J. Smith, C. Kosmidis, P. Tzallas, A.J. Langley, P.F. Taday, J. Phys. B: At. Mol. Opt. Phys. 32 (1999) 5557.
[24] D.J. Smith, K.W.D. Ledingham, R.P. Singhal, T. McCanny, P. Graham, H.S. Kilic, P. Tzallas, C. Kosmidis, A.J. Langley, P.F. Taday, Rapid Commun. Mass Spectrom. 13 (1999) 1366.
[25] C.Y. Wu, Q.H. Gong, Chin. Phys. 10 (2001) 814.
[26] S. Shimizu, J. Kou, S. Kawato, K. Shimizu, S. Sakabe, N. Nakashima, Chem. Phys. Lett. 317 (2000) 609.
[27] S. Couris, E. Koudoumas, S. Leach, C. Fotakis, J. Phys. B: At. Mol. Opt. Phys. 32 (1999) L439.
[28] S. Banerjee, G.R. Kumar, D. Mathur, Phys. Rev. A 60 (1999) R3369.